

# Zero-temperature responses of a 3D spin glass in a field

F. Krzakala<sup>1</sup>, J. Houdayer<sup>2</sup>, E. Marinari<sup>3</sup>, O. C. Martin<sup>1</sup> and G. Parisi<sup>3</sup>

<sup>1</sup> *Laboratoire de Physique Théorique et Modèles Statistiques, bât. 100, Université Paris-Sud, F-91405 Orsay, France.*

<sup>2</sup> *Institut für Physik, D-55099, and Max Planck Institut für Polymerforschung, D-55128 Mainz, Germany.*

<sup>3</sup> *Dipartimento di Fisica, INFN, SMC and INFN, Università di Roma La Sapienza, P. A. Moro 2, 00185 Rome, Italy.*

(October 31, 2018)

We probe the energy landscape of the 3D Edwards-Anderson spin glass in a magnetic field to test for a spin glass ordering. We find that the spin glass susceptibility is anomalously large on the lattice sizes we can reach. Our data suggest that a transition from the spin glass to the paramagnetic phase takes place at  $B_c \approx 0.65$ , though the possibility  $B_c = 0$  cannot be excluded. We also discuss the question of the nature of the putative frozen phase.

75.10.Nr, 75.40.Mg, 02.60.Pn

Ising spin glasses [1] have been studied intensively for over two decades; nevertheless, even the basic issue of the nature of the phase diagram is still unsettled. There are two main schools of thought in the long standing debate over whether a spin glass phase can exist in the presence of a magnetic field  $B$ . In the mean field picture [2] the spin glass phase exists up to some critical field value  $B_{AT}(T)$ , *i.e.*, up to the so called “de Almeida-Thouless” line [3] (AT) where replica symmetry breaking (RSB) arises. In the droplet picture [4,5], any non-zero magnetic field kills the spin glass ordering and makes the system paramagnetic.

Experimental evidence in favor of each school of thought has been claimed [6,7], but no consensus has emerged. On the computational side, the approaches using Monte Carlo have been hindered by the large finite size effects present in  $d = 3$  [8–10]. Because of this, dynamical out-of-equilibrium approaches have been used (*e.g.*, [11,12] for  $d = 4$  and [13,14] for  $d = 3$ ); those works hint at the existence of a phase transition in field, but it is preferable to have a direct test using a system *in* equilibrium. For such a test, one should stay away from the critical point at  $B = 0$ . To achieve this, we focus in this work on the  $T = 0$  line in the  $B$ - $T$  phase diagram; then the spin glass ordering can be tested through the behavior of excitations above the ground state.

We begin by discussing possible scenarios for the spin glass ordering when  $B \neq 0$ . In our first approach, we extract low energy excitations and investigate their size as a function of  $L$  and of  $B$ ; we also consider some of their topological properties. In a second approach, we compare ground states with periodic and anti-periodic boundary conditions, and extract a “magnetic penetration length”. We use extrapolations and finite size scaling to estimate the critical field  $B_c$  where the system becomes paramagnetic. Our results suggest  $B_c \approx 0.65$ .

*The model and spin glass ordering* — We consider the EA Hamiltonian on a 3D  $L^3$  periodic cubic lattice:

$$H_J(\{S_i\}) \equiv - \sum_{\langle ij \rangle} J_{ij} S_i S_j - B \sum_i S_i . \quad (1)$$

In this Edwards-Anderson (EA) model, the sum is over all nearest neighbor spin pairs,  $S_i = \pm 1$ , and  $B$  is the strength of the magnetic field. The quenched couplings  $J_{ij}$  are independent random variables taken from a Gaussian distribution of zero mean and unit variance. At  $B = 0$ , it is widely believed that the low  $T$  behavior of this system is characterized by a frozen but random ordering of the local magnetizations:  $\langle S_i \rangle \neq 0$ , where  $\langle \cdot \rangle$  is the thermal average. When  $B > 0$ , there is no up-down symmetry and the fact that  $\langle S_i \rangle \neq 0$  is not relevant. Instead, one relies on the correlation length  $\xi$ :  $\xi = \infty$  in the spin glass phase, whereas  $\xi$  is finite in the paramagnetic phase.

We study the system at  $T = 0$  and ask what signature corresponds to a  $\xi = \infty$  behavior of  $T > 0$  system. Given the ground state in the presence of  $B$ , consider droplet excitations, *i.e.*, excitations that are of minimal energy at fixed “size” (taken generally as the “radius”  $r$  of the connected cluster of spins that are flipped). Let  $\theta$  be the exponent [5] giving the characteristic excitation energy of these droplets:  $E \approx r^\theta$ . If the distribution of the rescaled energies,  $P_d(E/r^\theta)$ , has a non-zero density at zero argument, then there are enough thermally activated droplets of all sizes to make the correlation length infinite for low enough temperatures. We have three main scenarios:

(1) The “mean field” scenario: if  $B$  stays below some critical value  $B_{AT}$  there is RSB [2]; for  $B > B_{AT}$  the behavior is paramagnetic. Because of RSB, spin-spin correlation functions do not cluster when  $B < B_{AT}$ : any reasonable definition of  $\xi$  leads to  $\xi = \infty$  below  $B_{AT}$ .

(2) The “scaling/droplet” scenario: as soon as  $B > 0$  the system is paramagnetic. Motivation for this scenario comes from the large field limit: there,  $\theta = 3$  because excitation energies grow *linearly* with the number of spins flipped. Based on fixed-point arguments, one then expects  $\theta = 3$  and  $P_d(0) = 0$  for all  $B > 0$ . Because of this last property, large scale droplets cannot be thermally activated in the presence of a field (or equivalently when there is an extensive magnetization).

(3) An “intermediate” scenario: the spin glass order survives at positive  $B$ , but there is no RSB and thus no

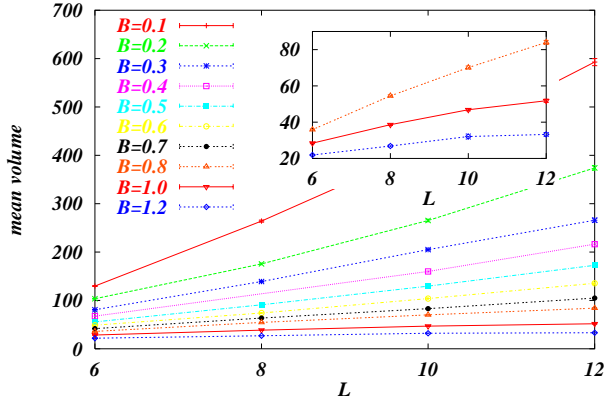


FIG. 1. Mean volume of the droplets extracted by the one-spin flip method as a function of  $L$ . From top to bottom:  $B = 0.1, 0.2, \dots$ . In the insert  $B = 0.8, 1.0$  and  $1.2$ .

AT line.  $\theta(B)$  may be arbitrary while  $B_c$  is defined as the field where  $P_d(0)$  goes to 0, separating the regime of  $\xi = \infty$  from the one where  $\xi < \infty$ . Since this scenario has large scale thermally activated droplets *co-existing* with an extensive magnetization, we will refer to it as the MAD (Magnetization And Droplets) scenario.

*Droplet sizes* — In our first approach we generate low energy clusters of spins according to a *one spin flip* method. Given the ground state  $C_0$  of  $H$ , we randomly choose a spin  $S_{i_0}$  and force its orientation to be opposite from what it is in the ground state. Then we recompute the new ground state  $C$  given this constraint. (The numerical algorithm for computing the ground states is described in [15].) The difference between  $C$  and  $C_0$  is a connected cluster of spins whose volume we denote by  $V$ ; it is the lowest energy cluster among all those containing  $S_{i_0}$ . The mean cluster size  $\langle V \rangle$  is analogous to the spin glass susceptibility  $\chi_{SG} = L^3 \langle (q - \langle q \rangle)^2 \rangle$ , where  $q$  is the standard spin overlap. A diverging  $\langle V \rangle$  as  $L \rightarrow \infty$  corresponds to a spin glass phase, while a bounded  $\langle V \rangle$  is the signature of a paramagnetic phase.

For each value of  $B$  ( $0.1 \leq B \leq 1.2$ , in steps of 0.1) we have generated 3000 disorder instances for  $L = 6, 8, 10$ , and 1000 for  $L = 12$ . In figure 1 we display the mean volume  $\langle V \rangle$  of the droplets generated by this one-spin flip method. (The spin  $S_{i_0}$  selected for flipping is chosen at random amongst the 25% spins with the largest local fields; this enhances the signal but does not affect our conclusions.) At  $B \geq 1$  we see signs of  $\langle V \rangle$  saturating when  $L$  grows: these large  $B$  values are in the paramagnetic phase. For smaller values of  $B$ ,  $\langle V \rangle$  grows significantly with increasing  $L$ . In the droplet picture there is a magnetic length  $\ell_B$  which acts as a cut-off:  $\langle V \rangle$  will grow as a power of  $L$  until  $L \approx \ell_B$ , and thereafter it will saturate. Furthermore, this cut-off length grows as  $B$  decreases,  $\ell_B \approx (\Upsilon/B)^{\frac{3-2\theta}{2}}$ . On the contrary, in the MAD and mean field scenarios  $\langle V \rangle$  diverges for all  $B \leq B_c$ .

Consider for example the data at  $B = 1.0$ . If we use

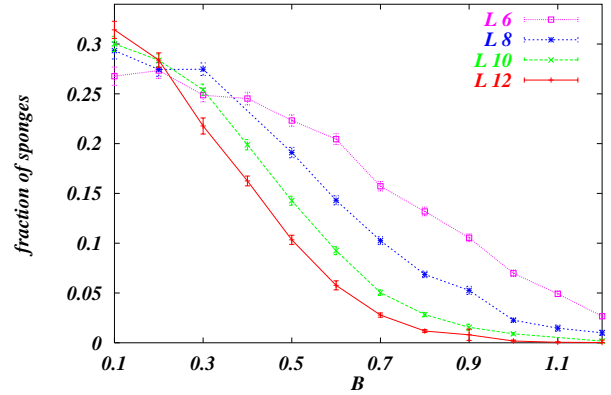


FIG. 2. Fraction of sponge-like excitations versus  $B$ .

the estimates on the largest lattices [16] available to date ( $\Upsilon \approx 1.78$  and  $\theta \approx 0.19$ ), we have  $\ell_B(B = 1.0) \approx 2.13$ .  $\langle V \rangle$  should be roughly the cube of this number, while we find  $\langle V \rangle = 52$  at  $L = 12$ . Such a large value of  $\langle V \rangle$  is unexpected in the droplet picture. Unfortunately, since the values of  $\Upsilon$  and  $\theta$  have large uncertainties, one cannot be more quantitative than that. In fact, the curves displayed in figure 1 could be interpreted either by saying that for  $B \leq 0.8$ ,  $\ell_B$  is comparable to our largest lattice sizes, or that  $\langle V \rangle$  diverges as  $L \rightarrow \infty$  even when  $B$  is not too small, for instance for  $B < 0.6$ . To further test the different scenarios, we follow [17] and focus now on the *topology* of our excitations.

*Fraction of sponge-like excitations* — In the mean field (RSB) picture, macroscopically distinct valleys differing by energies of  $O(1)$  arise with positive probability when  $B < B_{AT}$  and with zero probability for  $B > B_{AT}$ . (When the volume is finite, this last probability should go to zero exponentially in  $L$ .) These valleys differ by excitations that span the whole system and that *wind* around the lattice. We say that the cluster associated with one of our excitations is *sponge-like* if both it and its complement wind around all three directions  $(x, y, z)$  of the lattice. This motivates our measuring the fraction  $f(B, L)$  of the excitations generated by our one-spin flip method that are sponge-like. (For low field values, we observe that the flipped cluster sometimes contains more than  $0.5L^3$  lattice sites; since such events disappear as  $L \rightarrow \infty$  in all three scenarios, we have excluded them from our analysis in order to reduce the finite size corrections.) Let  $f^*(B)$  be the large  $L$  limit of  $f(B, L)$ .  $f^*(B)$  is an order parameter for RSB: it is zero for  $B > B_{AT}$  and positive for  $B < B_{AT}$ .

In figure 2 we show our values for the fractions  $f(B, L)$ . As expected at large  $B$ ,  $f$  goes to zero with increasing  $L$ . If there is RSB, the large  $L$  curves will converge to a limiting function that intersects the  $x$  axis at  $B_{AT} > 0$ . On the contrary, in the other pictures where replica symmetry is not broken, the limiting curve is  $f^*(B) = 0$

for all  $B > 0$ .

What can be said from these data within the RSB scenario? The order parameter should behave as  $f^*(B) \approx (B_{AT} - B)^\beta$  with  $\beta$  less or equal to its mean field value of 1. Thus we expect  $f^*$  to be convex for  $B$  not too close to 0. Now if we make the reasonable assumption that  $f(B, L)$  converges to  $f^*$  monotonically, then we get a bound on  $B_{AT}$  by taking the tangent to the  $L = 12$  curve; this leads to  $B_{AT} \leq 0.65$ . Of course, we can be more realistic and say that the curves for different  $L$  drift towards  $f^*$  in a smooth way. If we do that and extrapolate the curves by eye, we find  $B_{AT} \leq 0.4$ . Obtaining a less subjective estimate requires using finite size scaling and parametrizing  $f^*$ , but our small range in  $L$  makes such an attempt futile.

Consider now the data from the point of view of the two scenarios with no RSB. We have performed the finite size scalings  $f(B, L) = L^{-\beta/\nu} F[(B_c - B)L^{1/\nu}]$  where  $B_c = 0$  in the scaling/droplet scenario and  $B_c > 0$  in the MAD scenario. For each putative value of  $B_c$ , we first adjust  $\beta/\nu$  so that  $F$  is nearly  $L$  independent at  $B = B_c$ , and then we adjust  $\nu$  for the curves to superpose as well as possible. For both  $B_c > 0$  and  $B_c = 0$  the data collapse is far from perfect, so we cannot use the chi squared for a quantitative analysis. However, the quality of the superposition can be judged by eye. For  $B_c \approx 0$ , the superposition is reasonably good and leads to  $\nu = 1.25$  and  $\beta \approx 0$  (recall that sponges seem to arise with a finite probability in zero field). As  $B_c$  is increased, the superposition first becomes less good but then becomes better again at intermediate values with a local optimum at  $B_c \approx 0.65$ ; there we find  $\nu \approx 0.8$  and  $\beta \approx 2.0$ . Without a reliable parameterization of the finite size effects and larger lattice sizes, it is not possible to go beyond these qualitative conclusions.

*Periodic-anti-periodic computation* — In our second approach we perturb the couplings  $J_{ij}$  and probe how this affects the ground state. First we compute the ground state with periodic boundary conditions. Then we change the sign of all the  $J$ s cutting a given vertical plane  $\Pi$ ; this amounts to applying anti-periodic boundary conditions across this plane. Finally we re-compute the ground state for this new system. In contrast to the zero field case, gauge invariance is broken here and the plane  $\Pi$  where the  $J$ s are reversed is measurable. Our reason for choosing this particular perturbation is that it is translationally invariant in two directions; this leads to good statistics on the observables.

Given this “perturbation”, how does the difference between the two ground states look? At high fields, a few spins will be flipped in the immediate neighborhood of the plane  $\Pi$ . As  $B$  decreases, the region affected by the perturbation will broaden; one can introduce a “magnetic penetration length”  $\ell_P$  as a measure of the region’s width. In the paramagnetic phase,  $\ell_P$  is finite, while it is plausible that it grows with the system size  $L$  in a

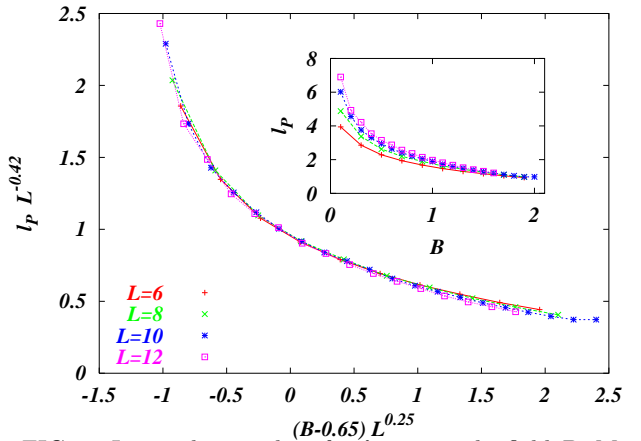


FIG. 3. Inset: the raw data for  $\ell_P$  versus the field  $B$ . Main plot:  $\ell_P$  rescaled by  $L^{-0.42}$  versus rescaled distance from  $B_c$ .

spin glass phase. It is possible that in a droplet picture  $\ell_P = \ell_B$ , but we do not develop this issue here.

To define  $\ell_P$  from the perturbed region, we measure the spin-spin overlap of the two ground states and then average in each plane parallel to  $\Pi$ . Let  $Q(d)$  be this overlap, with  $d$  the distance from  $\Pi$ . In the paramagnetic phase  $Q(d)$  will go to 1 at large  $d$ , and the approach to this asymptote should go as  $\exp(-d/\ell_P)$ . If on the contrary  $\ell_P = \infty$ , the asymptote may be different from 1, and the approach to that value can be a power law in  $d$ . For each  $L$  and  $B$  we extract  $\ell_B$  by fitting  $Q(d)$  to the form  $1 + A \exp(-d/\ell_B)$ . Above  $B_c$ , this should lead to the measurement of the true  $\ell_B$ , while below  $B_c$  the extracted  $\ell_B$  will be an effective length that will grow with  $L$ . (In these measurements, we used 40000 disorder samples at  $L = 6$  and 20000 at  $L = 8$  for each  $B$ ; for  $L = 10$ , we used 5000 samples at the smallest  $B$  value and up to 12800 on the largest one, while we used from 1000 to 7000 samples for  $L = 12$ .) The fits performed using all the distances gave results very similar to the ones using only the four (symmetrized) data points at the largest values of  $d$ .

We show the results of our best fits in the inset of figure 3.  $\ell_P$  saturates at high fields, while it increases with  $L$  at low field. We also show in the figure a finite size scaling plot in which we have set  $B_c = 0.65$ ;  $\ell_P$  has been rescaled by  $L^{-0.42}$  and  $(B - B_c)$  by  $L^{0.25}$ . The data collapse is good, but similarly good results are obtained for all values of  $B_c < 1.0$ ; the problem is that when data do not have a big dynamic range, finite size scaling can almost always be made to work. Thus for this method we have no precision on the estimate of  $B_c$ .

We have also used other methods to estimate  $\ell_P$  from the set of spins that are flipped in the periodic-anti-periodic transformation; these include the set’s mean distance to  $\Pi$ , the mean extension of its interface, etc... All these measures lead to  $\ell_P$  comparable to  $L$  when  $B \leq 0.7$  for our range of  $L$ s. It is thus difficult for us to say

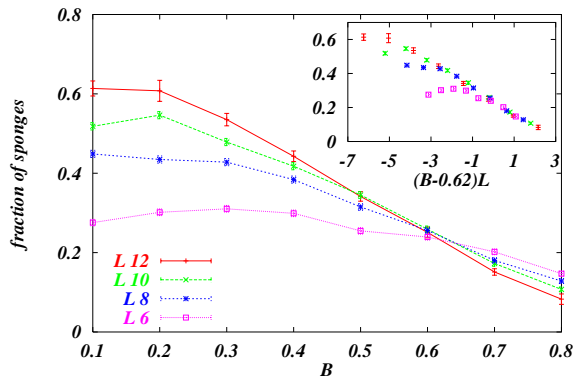


FIG. 4. Fraction of *sponge-like* clusters in the periodic anti-periodic approach. The insert gives the best finite size scaling fit ( $B_c = 0.62$ ,  $\nu = 1.0$ ).

whether  $\ell_P$  diverges when  $B$  reaches  $B_c > 0$  or only when  $B \rightarrow 0$ , but this is not unexpected, and has been a serious shortcoming in all attempts to detect a spin glass ordering in a field. Because of this, we now again appeal to topology: we measure the proportion of instances where the flipped spins form a sponge-like cluster.

The raw data for the fraction of sponges are plotted in figure 4. We observe a crossing point, suggesting a first order jump in this fraction at  $B_c \approx 0.65$ . This is probably our clearest evidence for the existence of a spin glass phase with  $B_c > 0$ . To perform finite size scaling, we take the fraction of sponge-like events to be a function of  $(B - B_c)L^{1/\nu}$ ; the best data collapse is obtained for  $B_c \approx 0.62$  and  $\nu \approx 1.0$  and is displayed in the figure's insert. (Note that the data at low  $B$  goes to the limiting curve only slowly when  $L$  increases.) These data are compatible with a  $B_c \approx 0.65$ ; however, since the crossing points drift a bit, a smaller value for  $B_c$  cannot be ruled out.

*Discussion* — We have introduced and exploited a new approach for testing whether a spin glass ordering arises in the presence of a magnetic field. The major advantage of our method compared to Monte Carlo is that since we work at  $T = 0$ , we are far from the  $B = 0$  critical point,  $T_c \approx 0.95$ . Our main conclusion is that very plausibly in three dimensions, a spin glass phase survives up to a critical field  $B_c \approx 0.65$ ; beyond that, the system becomes paramagnetic.

Our proposed value is several times smaller than the mean field value [18],  $B_{AT}^{MF} \approx 2.1$ . Such a low value for  $B_c$  makes it difficult to establish without ambiguity that  $B_c > 0$ . This problem is analogous to the difficulty of showing that  $T_c > 0$  in  $d = 3$  spin glasses; to give plausible evidence, finite size effects must be under excellent control. Clearly, that is not yet the case here, but the fact that our different approaches lead to consistent values of  $B_c$  gives some strength to our findings.

Finally, there is the question of a possible replica symmetry breaking transition at  $B_{AT} > 0$ . Our numerical

study leads us to suggest that  $B_{AT} \leq 0.4$  if it is indeed positive. This very low value is compatible with the findings of [13]. However, confirming such a value via equilibrium measurements will require larger lattice sizes than we can handle at present.

*Acknowledgments* — We thank M. Mézard, E. Vincent and F. Zuliani for stimulating discussions. F.K. acknowledges financial support from the MENRT and J.H. from the Max Planck Institute für Polymerforschung. E.M. acknowledges an IUF visiting professorship at Orsay during the early part of this work and a travel grant from the ESF SPHINX program. E.M. and G.P. acknowledge support from the INFM *Center for Statistical Mechanics and Complexity* (SMC). The LPTMS is an Unité de Recherche de l'Université Paris XI associée au CNRS.

- 
- [1] *Spin Glasses and Random Fields*, edited by A. P. Young (World Scientific, Singapore, 1998).
  - [2] M. Mézard, G. Parisi, and M. A. Virasoro, *Spin-Glass Theory and Beyond*, Vol. 9 of *Lecture Notes in Physics* (World Scientific, Singapore, 1987).
  - [3] J. R. L. de Almeida and D. J. Thouless, *J. Phys. A* **11**, 983 (1978).
  - [4] A. J. Bray and M. A. Moore, *J. Phys. C Lett.* **17**, L463 (1984).
  - [5] D. S. Fisher and D. A. Huse, *Phys. Rev. Lett.* **56**, 1601 (1986).
  - [6] A. Ito and H. A. Katori, *J. Phys. Soc. Japan* **63**, 3122 (1994).
  - [7] J. Mattsson *et al.*, *Phys. Rev. Lett.* **74**, 4305 (1995).
  - [8] S. Caracciolo, G. Parisi, S. Patarnello, and N. Sourlas, *Europhys. Lett.* **11**, 783 (1990).
  - [9] E. R. Grannan and R. E. Hetzel, *Phys. Rev. Lett.* **67**, 907 (1991).
  - [10] N. Kawashima and N. Ito, *Jour. Phys. Soc. of J.* **62**, 435 (1993).
  - [11] G. Parisi, F. Ricci-Tersenghi, and J. Ruiz-Lorenzo, *Phys. Rev. B* **57**, 13617 (1998).
  - [12] E. Marinari, G. Parisi, and F. Zuliani, *J. Phys. A* **31**, 1181 (1998).
  - [13] E. Marinari, G. Parisi, and F. Zuliani, *Phys. Rev. Lett.* **84**, 1056 (1999), cond-mat/9812401.
  - [14] E. Marinari, G. Parisi, and F. Zuliani (unpublished).
  - [15] J. Houdayer and O. C. Martin, *Phys. Rev. E* **64**, 056704 (2001), cond-mat/0105617.
  - [16] M. Cieplak and J. Banavar, *J. Phys. A.* **23**, 4385 (1990).
  - [17] J. Houdayer, F. Krzakala, and O. C. Martin, *Eur. Phys. J. B.* **18**, 467 (2000), cond-mat/0009382.
  - [18] J. Houdayer and O. C. Martin, *Phys. Rev. Lett.* **82**, 4934 (1999), cond-mat/9811419.